iodomethane, CO, H_2, where the molar ratio of CO to H_2 varies from 1:1 to 1:6. The reaction is conducted as a continuous process at a temperature between 90-250°C and a pressure between 20-70 atmospheres. From the analytical data shown, there appears to be a greater yield and selectivity towards acetic acid. The second patent shows a way of supporting the same catalyst on a phosphinated DVB-PS resin as shown by the reaction scheme below.
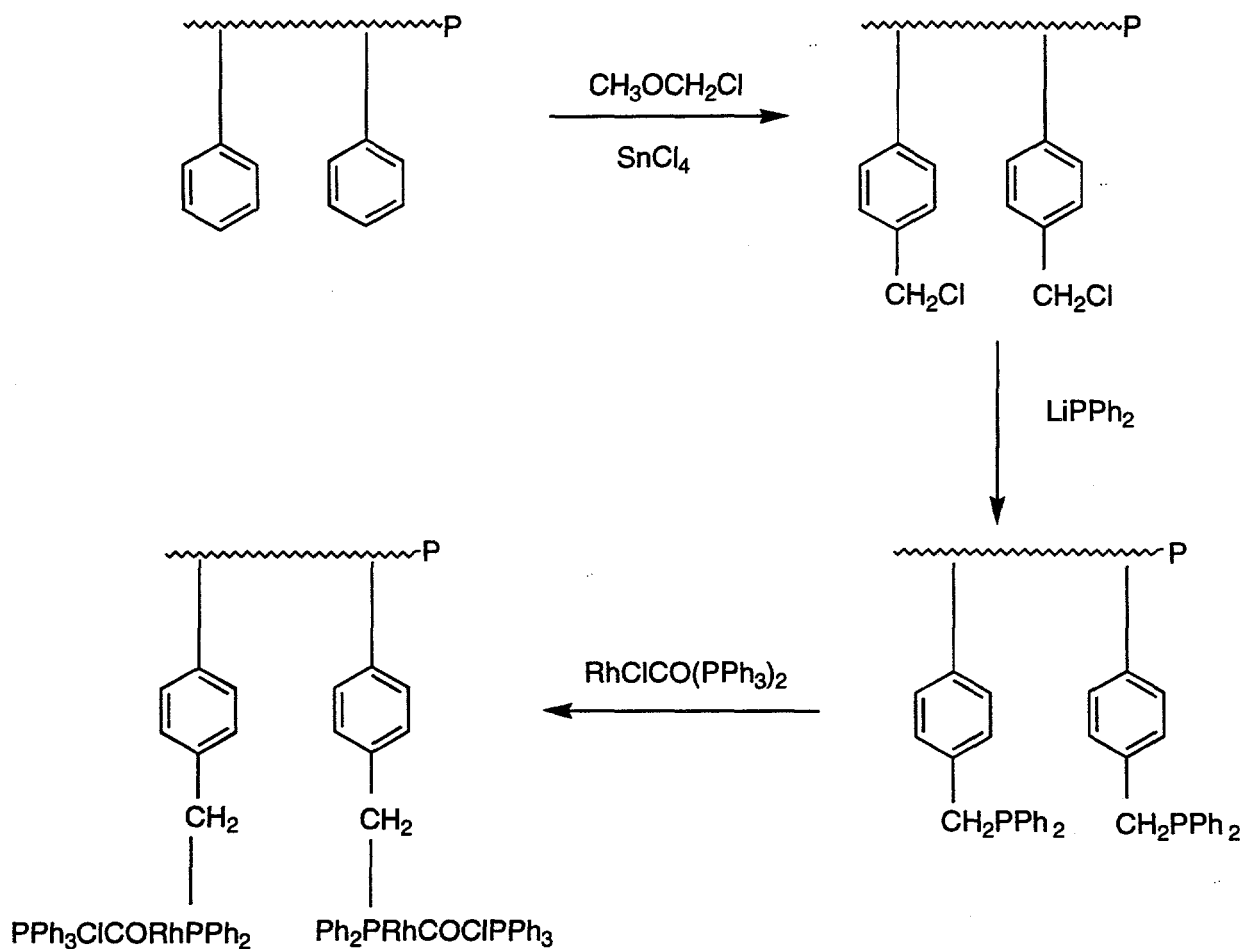

An accelerator such as 3-picoline was added to facilitate the catalytic reaction. The feed gases and reaction conditions were the same as those used for the alumina supported catalyst, and though EDA was produced, acetic acid was a major product.

Catalyst Preparation and Characterization
A sample of Reillex 425 polymer was obtained from Reilly Industries. This polymer is made by crosslinking 4-vinylpyridine with divinylbenzene, and is available as off-white beads that are thermally stable up to 260°C. The beads as obtained are wet, with a water content of 50-60%. Approximately 24g of the Reillex 425 were dried in a regular oven at 90°C for 12 h. To these beads were added ~125ml of toluene, and the mixture was refluxed for 30 min. under nitrogen. The beads were observed to expel the trapped air and then sink to the bottom of the flask. After the mixture cooled to room temperature, 20 ml of methyl iodide were added, at which time the

beads were observed to turn pale yellow. The solid was filtered and dried under vacuum. The actual reaction is described by the equation shown below.
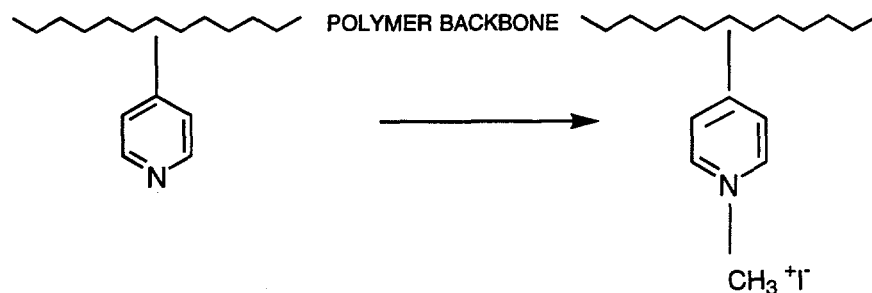
The solid was characterized by solid state ^{13}C nmr. The spectrum of the Reillex 425 shows a strong signal at 40 ppm due to the hydrocarbon backbone of the polymer. After the reaction with methyl iodide, the spectrum shows a new shoulder at 50 ppm due to the methyl group on the pyridine. Also it can be seen that the aromatic carbons at 130 and 150 ppm are shifted closer together. This is further evidence that the nitrogen on the pyridine has been alkylated. However, it does not tell how many free pyridines are left over at the end of the reaction.

The next step of the reaction was to load the Reillex polymer with a rhodium complex by the reaction shown below:
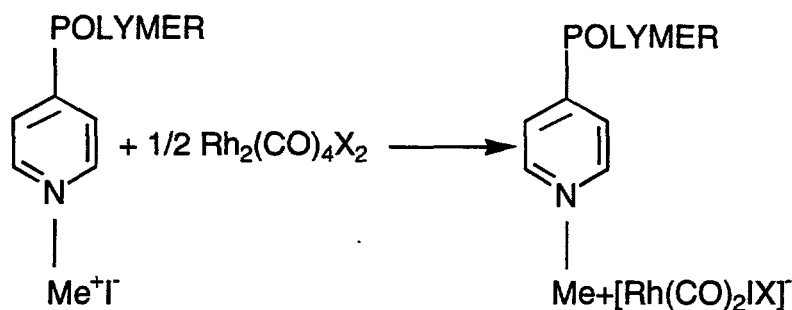
Approximately 4g of the alkylated Reillex were added to a solution of 0.18g $Rh_2(CO)_4Cl_2$ in 100 ml of toluene. Immediately, the yellow color of the solution dissipated and the yellow Reillex became more orange. If all of the rhodium incorporated, this would amount to a 2.375% loading. However, the actual loading can only be found by an elemental analysis. An infrared spectrum of the solid now showed two characteristic carbonyl bands at 2056, 1983cm^{-1}, which corresponds well with the literature values of the tetraphenylarsonium $[Rh(CO)_2I_2]$ at 2060 and 1988cm^{-1}.

Catalyst Testing

The catalytic performance of the heterogeneous catalyst was compared with the analogous homogeneous system using similar experimental conditions (syn gas, 190°C, 1500 psi).

Test 1 - Homogeneous Catalysis Without Lithium Iodide

Reaction conditions were 0.2 g $RhCl_3.3H_2O$, 8.13 g DME, 9 g methyl iodide, 143.7 acetic acid, syn gas (50:50), 190°C, 1500 psi. The results are shown in Figure 3.2.5.

Figure 3.2.5. Hydrocarbonylation of DME with a Homogeneous Rhodium Catalyst without LiI
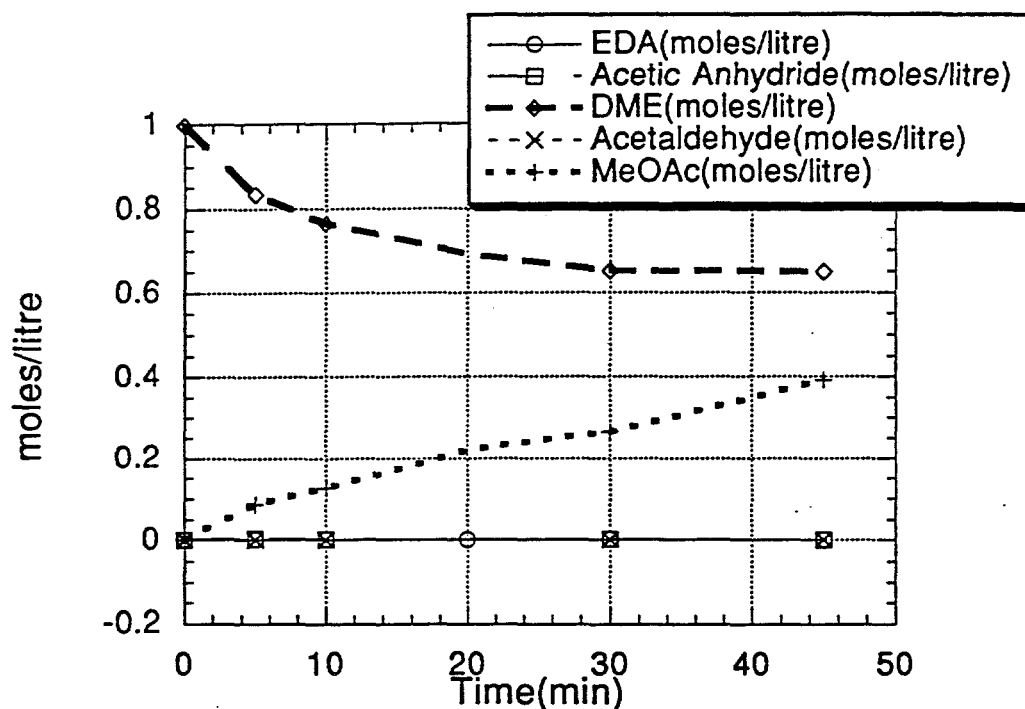
It can clearly be seen that over a period of 45 min. the DME concentration decreases while the methyl acetate concentration builds up. However, no products in the form of acetic anhydride, acetaldehyde or ethylidene diacetate were seen.

Test 2 - Heterogeneous Catalysis Without Lithium Iodide

Reaction conditions were 1.47g Reillex containing 2% Rh, 10.87g DME, 9g methyl iodide, 145.46g acetic acid, syn gas (50:50), 190°C, 1500 psi. The results are shown in Figure 3.2.6.

Figure 3.2.6. Hydrocarbonylation of DME with a Heterogeneous Rhodium Catalyst without LiI
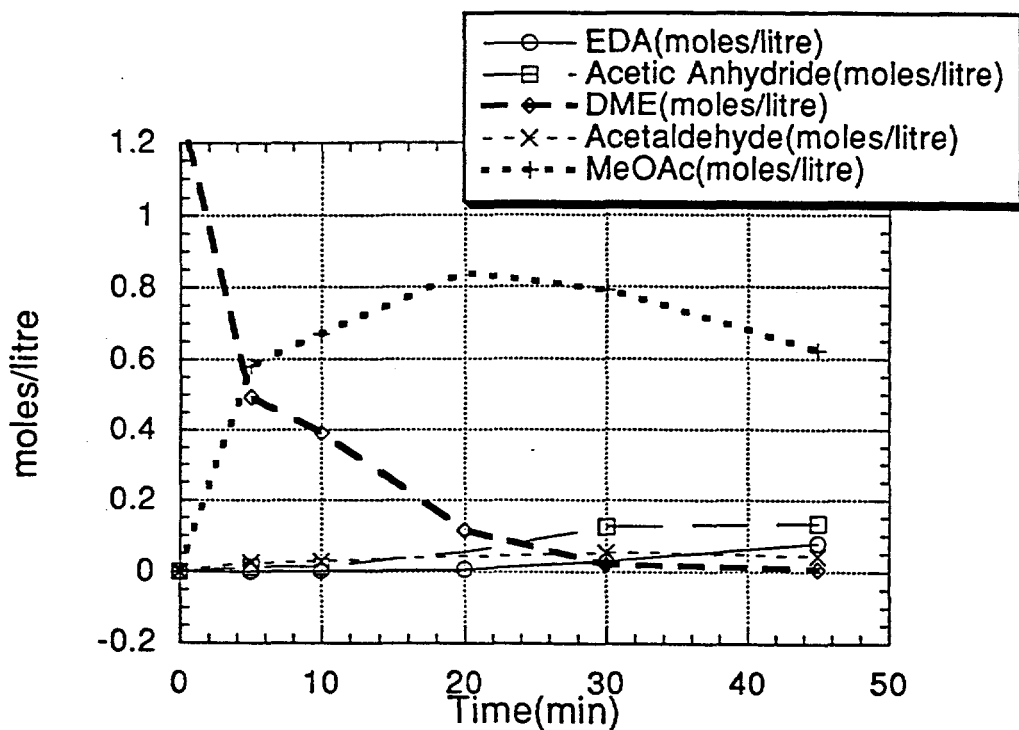

It can clearly be seen in the plot shown above that the heterogeneous catalyst behaves much better than the homogeneous one (test 1). The DME concentration drops rapidly and is almost completely consumed by the end of 45 minutes. The methyl acetate concentration builds up until the 20 min. mark, after which it drops presumably because the carbonylation rate now exceeds the rate of formation. The time axis also shows that between the 30 and 45 minute mark, a significant concentration of products (acetic anhydride, acetaldehyde, EDA) is seen.

At the 5 minute mark, the acetaldehyde concentration is higher than the acetic anhydride concentration. This must mean that there is another mechanism for the formation of acetaldehyde directly from methyl acetate, in addition to the expected conversion of acetic

anhydride to acetaldehyde via hydrogenation. At the 20 minute mark we see the first signs of product EDA, and this rises steeply up to the 45 minute mark. Both the rates of formation of acetaldehyde and acetic anhydride are observed to decrease at the 30 minute mark, presumably because they are reacting together to form the product EDA.

The catalyst sample was analyzed for rhodium before and after the catalytic run to see if there was extensive leaching of the catalyst. The sample before the test run gave a 2% Rh analysis, while the sample after the test run gave a 1.63% Rh analysis. Based on these results we do not feel that there has been extensive leaching of the catalyst. The small difference in analysis may simply be due to further incorporation of methyl iodide into the polymer via reaction with pyridine groups, which will increase the weight of the polymer and reduce Rh analysis slightly. We plan to further test this hypothesis by doing successive catalytic runs using the same batch of material.

Test 3 -Heterogeneous Catalysis With Lithium Iodide

Reaction conditionswere the same as those for Test 2, except that 1.5g of LiI was added. The results are similar to those obtained with Test 2, and the added LiI did not show any advantage. In fact it proved to be a disadvantage as we observed major leaching of catalyst from the polymer. The Rh analysis was 0.55% after the run compared to 2% before the run. This is not unexpected since the iodide ions from the LiI could exchange with the anionic Rh complex.

Test 4 - Homogeneous Catalysis With Lithium Iodide

Reaction conditions were 0.2g $RhCl_3.3H_2O$, 9.9g DME, 9g methyl iodide, 1.49g LiI, 0.81g LiOAc, 146.8g acetic acid, syn gas(50:50), 190°C, 1500 psi. The results are shown in Figure 3.2.7.

Figure 3.2.7. Hydrocarbonylation of DME with a Homogeneous Rhodium Catalyst with LiI
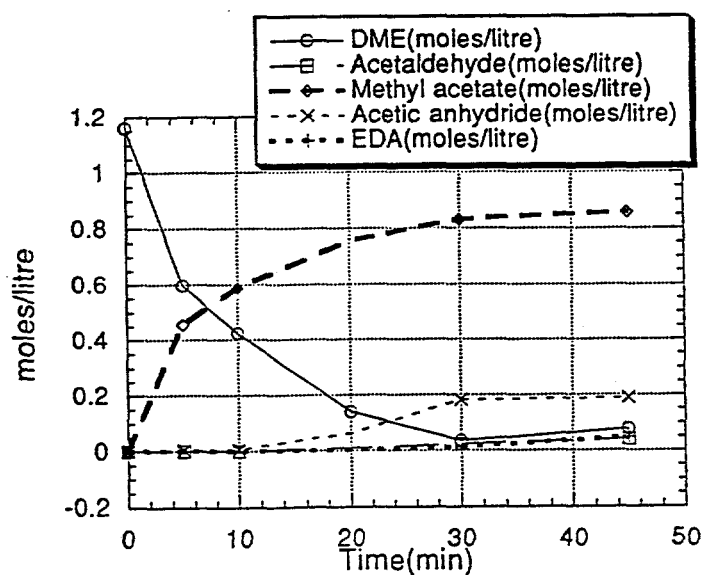
The addition of LiI and LiOAc to the homogeneous reaction does make the product EDA in contrast to Test 1, where no product was obtained. However, this reaction does not work as well as the heterogeneous reaction (Test 2), even though the homogeneous reaction yielded twice the amount of Rh by weight.

(iii) Nothing to report this quarter.

3Q FY95 Objectives

Future plans for Task 3.2 will focus on the following areas:

- Continue to screen immobilized catalyst candidates for hydrocarbonylation of dimethyl ether to ethylidene diacetate
- Determine the extent of any catalyst leaching from the best candidate
- Initiate catalyst development work on the cracking of ethylidene diacetate to vinyl acetate and acetic acid.

3.3   New Processes for Alcohols and Oxygenated Fuel Additives

3.3.1. Isobutanol Synthesis in a Three Phase System (RWTH Aachen)

Fixed Bed Reactor Design and Runs
The results from the fixed bed reactor were improved compared to those of the last quarter, paralleling the results reported by Falter. These results are provided in Figure 3.3.1.1:

Figure 3.3.1.1 Results from Catalytic Tests in the Fixed Bed Reactor
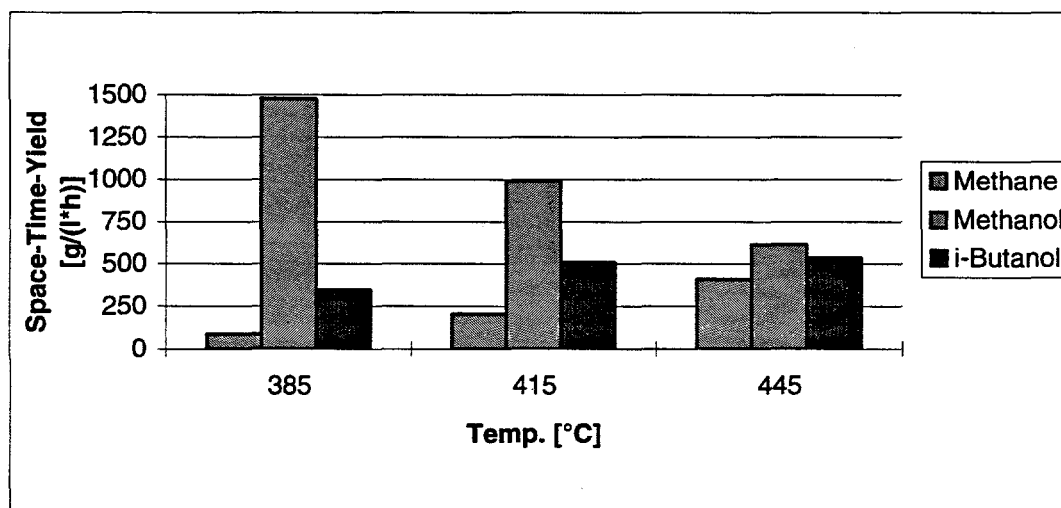
Pressure: 25 MPa
GHSV: 20000 h^{-1}
Catalyst: $ZrO_2/ZnO/MnO/K_2O/Pd$ (pH 9)

These improvements were achieved by changes in catalyst synthesis and the reduction of catalyst poisons. Former catalytic tests revealed a significant activity towards methane. These unexpected results led to the investigation of the presence of catalyst poisons. Surface analysis of catalyst pellets after reaction by x-ray fluorescence indicated iron and nickel impurities. In contrast, fresh catalysts were free of these impurities.

Consequently, the syngas was checked for iron pentacarbonyl by IR and indeed showed the expected peaks. The filter material used, a 4Å molecular sieve, was not able to adsorb iron pentacarbonyl. By using activated carbon as the filter material, the space time yield to methane was reduced more than ten times with respect to former runs. Since activated carbon was used as the filter material, the fixed bed results were improved and the influence of the temperature gradient at the reactor top was diminished. Best results were found without a temperature gradient.

It was observed that the reactor itself set nickel and iron free by corrosion. The roughness-height of the fixed bed reactor was considered to be the cause. Instead of reaming the fixed bed reactor used to date, a new reactor was made with a very smooth inner surface. A comparison between this new reactor and the one used by Falter showed quite similar results for isobutanol and methanol; in addition methane production in the new reactor was reduced another 50%.

Slurry Reactor Design and Runs
Two runs under the same reaction conditions were made using the slurry reactor, which could be connected to the unit without other modifications. On-line GC, product sampler and process management systems were run as if the fixed bed reactor would be used. The results from the slurry reactor can be compared directly to those obtained with the fixed bed reactor. The reaction conditions are listed in Table 3.3.1.1:

Table 3.3.1.1 Reaction Conditions for the Slurry Reactor

Temperature	400°C
Pressure	25 MPa
Mass flow	100 Nl/h (Syngas)
Catalyst	8 g powdered BASF "Isobutylölkatalysator"
Inert liquid	200 ml Decalin
Number of revolutions	1000 rpm

Methanol production was halved compared to the fixed bed reactor. Isobutanol production was about six times smaller. Decalin was found to be stable. It should be mentioned that these initial runs mainly served to check the unit's characteristics.

Due to the high vapor pressure of decalin, a complete separation of decalin and the reaction products in the reflux condenser seems impossible. Within 40 hours the amount of decalin in the reactor decreased. It seems necessary to recirculate the decalin after phase separation using a high pressure pump.

Future objectives are optimization of the slurry reactor and further tests with the catalysts mentioned under slurry conditions.

On-Line Screening

For injecting the samples without pressure, a different gas switching mode was designed. A better reproducibility of the of the on-line results has thus been achieved. In this way the maximum error has been minimized to a value smaller than 5%.

Catalyst Preparation

To improve the knowledge of the $ZrO_2/ZnO/MnO/M_2O/[Pd]$ (M: Li, K)[1] -type catalysts, one main objective has been the analysis of these catalysts. For this purpose they have been investigated using the following methods[2]:

AAS/XRF: The quantitative analysis by AAS was inaccurate because the measurement of zirconium is influenced by potassium. Nevertheless, this analysis showed that the samples precipitated with potassium at pH 9, 10 and 11 (BJ 27, 26, 31) were identical in their zinc and manganese content, but different in their potassium content. The calibration of the XRF-spectrometer has almost been completed. First results confirm the similarity in zinc, manganese and zirconium content.

Nitrogen Adsorption: The determination of BET- surfaces and porous structures showed surfaces of ca. 130 m^2/g and porous maxima in the range of 40-80 Å for all samples. Nitrogen adsorption has not yet been measured for palladium impregnated catalysts.

XRD: All catalysts were mainly amorphous. The observed crystalline phases were absolutely similar. So far these phases seem to be $Zn_2Mn_4O_8 \cdot H_2O$ (Hydroheterolyte), $ZnMn_2O_4$ (Heterolyte), $Zn(OH)_2$ (Ashoverite), Mn_3O_4 (Hausmannite) and Zn_2MnO_4. No crystalline phases of pure zinc- or manganese-oxides and only very small amounts of crystalline zirconium oxide could be identified.

DSC/TG[3]: In correspondence with the results mentioned, the thermogravimetric analysis revealed similar characteristics for the different catalysts, showing a slow loss of capillary- and surface water up to a temperature of 450-500°C and an exothermic effect without mass-loss (probably a phase transformation of zirconium oxide) at 650-690°C.
Typical examples of the analysis data are depicted in the appendix.

Conclusions drawn from these results are as follows:
- A precipitation pH ranging from 9-11 does not seem to affect the composition (excluding the alkaline content), surface, porous structure and crystallinity of the $ZrO_2/ZnO/MnO/M_2O$ (M: Li, K)- catalysts.

---

[1]All catalysts were calcined in flowing air at 330°C, with a heating rate <5°/min.
[2]Analysis has been completed for the potassium-containing catalysts. The results from the lithium-catalysts so far obtained confirm all statements.
[3]DSC / TG measurements have been made from the dried (130°C) but uncalcined catalysts

- Conclusions concerning the composition of the amorphous phases and the oxidation states of the transition metals cannot be drawn.
- So far the only perceivable difference between these catalysts is the alkaline content. This observation could be related to the differences in catalytic behavior.

Coprecipitated Alkaline Free Catalysts

The most direct way of studying the influence of alkaline metals in the Falter system is a precipitation followed by a washing procedure and subsequent impregnation. This can be done by washing with distilled water and measuring the conductivity of the washing water. As a first step, alkaline-free catalysts based on the precipitation with potassium hydroxide at pH 9 and 11 were prepared. Analysis showed absolute similarity to the alkaline-containing samples.

These catalysts will be impregnated with defined amounts of potassium acetate, calcined a second time and tested in catalysis. First, this will enable us to investigate whether there is any influence introduced through coprecipitation at different pH-levels. Similar behavior in catalysis after impregnation with the same amounts of potassium would confirm the analytic results. Second, this provides a way to optimize catalysts concerning their alkaline content.

Falter also obtained excellent results with catalysts prepared from different first and second main group metal bases. Therefore the following tests would be interesting if the above mentioned experiments are successful:
- Impregnation with different first and second main group metals instead of potassium in order to compare the influence of different bases.
- Precipitation with different first and second main group bases at several pH values, followed by washing them alkaline free. These catalysts could be impregnated with the same alkaline base to clarify whether the major influence of the alkaline base is exerted during precipitation or only by the absolute amount present.

Impregnation with Pd(acac)$_2$

The impregnation step with Pd(acac)$_2$ in acetonitrile was pointed out by Falter to increase both activity and selectivity to isobutanol. This impregnation step is performed by using a static impregnation method, leaving the catalyst pellets in an acetonitrile solution (30 ml) of Pd(acac)$_2$ (2.5 mg Pd/g catalyst). After decoloration of the yellow solution (3-14 days), the catalyst is filtered from the solution and calcined. In the case of catalysts $ZrO_2/ZnO/MnO/K_2O$ (BJ 26, 27, 31) a white, crystalline solid was observed on the catalyst surface after filtration. This solid seemed to decompose during calcination. In one case (BJ 27), the solid was separated from the catalyst by sieving. Analysis of the solid indicated that it contained mainly potassium. Interestingly this catalyst was one of the best in catalytic runs.

For this reason it will be necessary to investigate the impregnation in further detail to determine if this step affects only the palladium content or the alkaline content, as well.

Coprecipitation by Amine Bases

Apart from the influence of the alkali content, the precipitating agent is another parameter that may influence catalyst characteristics. This influence was investigated by using amine bases

instead of alkali hydroxides. In particular, precipitations were performed with ammonia and tetramethylammoniumhydroxide as bases at constant pH levels of 7 and 8, respectively. At high pH levels, dissolution of the metalhydroxides as amine complexes can occur, which will alter the composition. After synthesis the precipitates were washed free from remaining ammonium salts. Subsequently, these catalysts will be impregnated with alkalimetal, being indispensable for higher alcohol synthesis. So far, first characterization results (TG, XRD, BET) resemble those of the alkali precipitated catalysts.

Catalyst Synthesis by Complexation

Apart from coprecipitation, several other catalyst synthesis procedures are being investigated. Complexation is a method that avoids the usual imperfections of coprecipitation methods. It permits the production of amorphous solid compounds with a vitreous structure and a homogeneous composition, without a phase separation from the starting solution. This is achieved by evaporating a solution containing various metallic salts and a complexing agent, generally an -hydroxyacid. Following this route, several catalysts have been prepared. The currently used method will be optimized further.

Catalyst Synthesis by Sol-Gel Methods

Another field that has attracted considerable interest is sol-gel synthesis. Sol-gel processing can offer many advantages for catalyst design:

    purity
    homogeneity
    high thermal stability
    low-temperature processing

The sol-gel process can be described by two simplified chemical reactions: hydrolysis and polycondensation. Both reaction steps can occur in parallel, depending on reaction conditions. Small variations in, for example, precursor concentrations and water/alkoxide ratios can lead to formation of precipitates instead of clear homogeneous sols. Addition of bidentate ligands as acetylacetonate or glycol can prevent precipitation. Acetic acid has been successfully used as well. This method is currently being investigated for the synthesis of $ZrO_2/ZnO/MnO$ and $TiO_2/ZnO/MnO$ catalysts using zirconium and titanium alkoxides as precursors. Specific characterization data will be given in the next report.

Further Developments

The crystalline zinc-manganese phases in the $ZrO_2/ZnO/MnO$ catalysts observed in XRD-spectra could play an important role in the activity and selectivity of these systems. To test this hypothesis, a set of catalysts based on the system $M_xO_y/ZnO/MnO$ is being prepared, where zirconia has been exchanged against titanium, lanthanum or ceria. Several synthesis routes are being examined and will be followed by impregnation with alkali metals.

Appendix

Figure 3.3.1.2. Adsorption Isotherm of Catalyst BJ27

Sample: BJ 27 N2 F C 0.3 Jäger
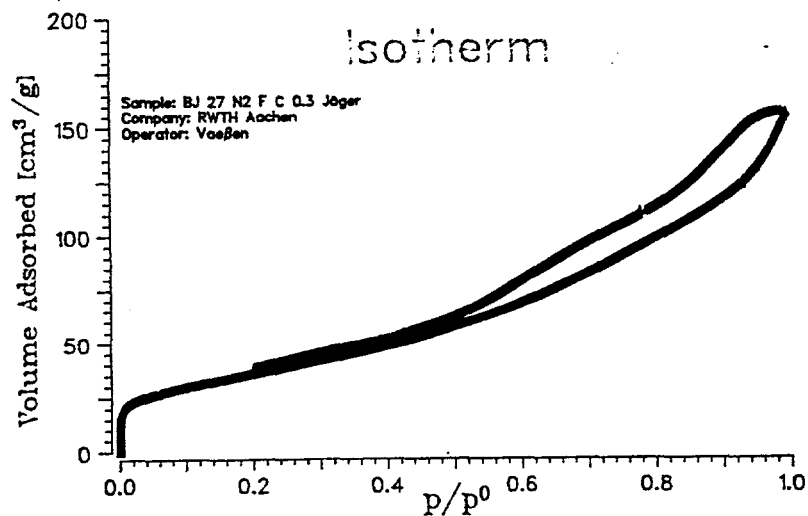Company: RWTH Aachen
Operator: Voeßen

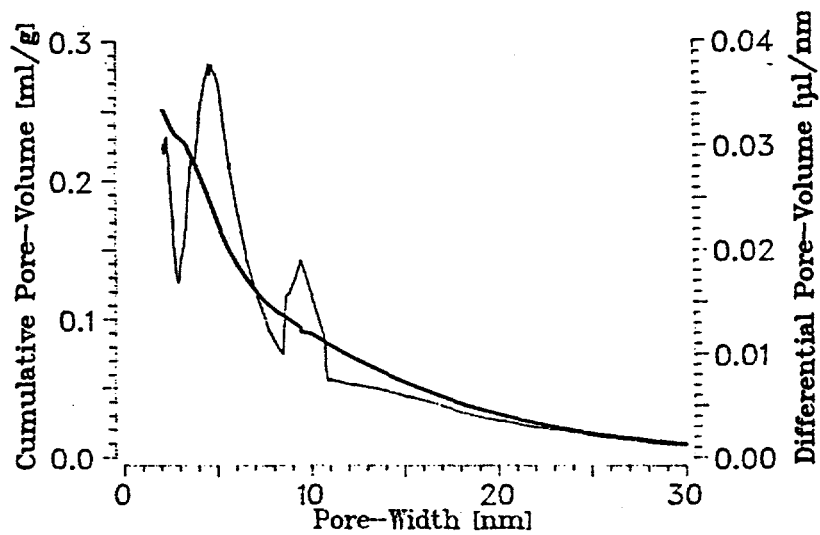## Figure 3.3.1.3. Pore Size Distribution of Catalyst BJ27

Figure 3.3.1.4. XRD Scan of Catalyst BJ27
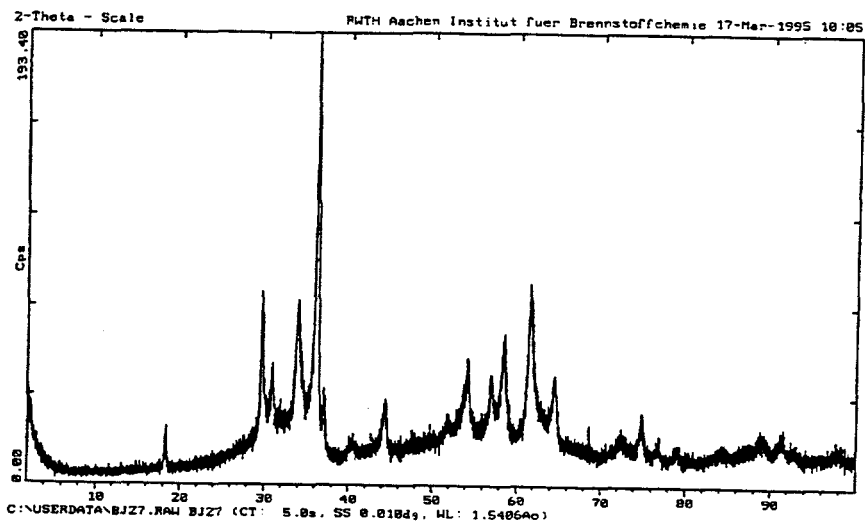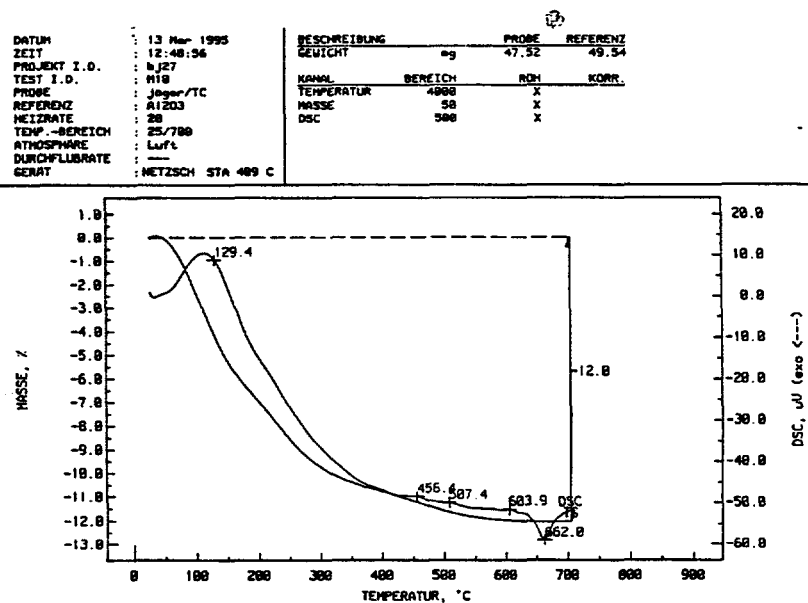

Figure 3.3.1.5. DSC/TG of Catalyst BJ2700

3.3.2 Oxygenates via Synthesis Gas (Lehigh University)

Introduction

During the previous quarter, it was shown that the $Cs/Cu/ZnO/Cr_2O_3$ catalyst was an active alcohol synthesis catalyst at the severe reaction temperature of 340°C, producing 45 g isobutanol/kg cat/hr and 138 g methanol/kg cat/hr. However, some deactivation toward higher alcohols occurred over a period of $\approx$250 hr. At the same time, the productivity and selectivity toward methanol increased. This quarter, research with this catalyst has focused on (i) the stability of the catalyst at the high reaction temperature of 340°C in $H_2/CO = 0.45$ synthesis gas and (ii) the effect of contact time and pressure on the productivity of the alcohol from $H_2/CO = 0.75$ synthesis gas at 325°C.

New Processes for Mixed Alcohols and Other Oxygenates

I.   Overall 2QFY95 Objectives

   (i)   To continue studies of increasing the surface area and catalytic activity of $Cs/Cu/ZnO/Cr_2O_3$ catalysts for higher alcohol synthesis from H_2/CO synthesis gas

   (ii)   To prepare and test high surface area Cu/ZrO_2 catalysts that are candidates for the synthesis of C_1-C_5 alcohols, in particular branched products such as isobutanol, and

   (iii) To make substantial progress in establishing the accessibility, number, and type (Lewis or Bronsted) and strength of the active surface acid sites by volumetric and HR-XPS analyses after pyridine adsorption on the sulfated zirconia catalyst that is highly active for the selective dehydration of isobutanol to isobutene from methanol/isobutanol reactant mixtures.

Results and Discussion

The preparation, characterization, and testing of catalysts this quarter has centered on oxide catalysts for alcohol synthesis from H_2/CO synthesis gas mixtures. The particular catalysts studied are based on $Cu/ZnO/Cr_2O_3$ and Cu/ZrO_2, and an introduction to the former catalyst, with and without the presence of CsOOCH dopant, was provided in the previous quarterly report.

The preparation of the $Cu/ZnO/Cr_2O_3$ catalyst was described in the previous report, and it was doped with an aqueous CsOOCH solution under a N_2 atmosphere to yield a 3 mol% $Cs/Cu/ZnO/Cr_2O_3$ catalyst. A portion of this catalyst was previously tested in the high temperature range of 310-340°C as a function of the temperature and H_2/CO molar ratio in the reactant mixture. During the present quarter, additional studies have been carried out at 325 and 340°C.

The 3 mol% $Cs/Cu/ZnO/Cr_2O_3$ catalyst has been tested at the severe reaction temperature of 340°C as part of any accelerated stability test. The purpose of the experiment was to follow the

catalyst activity (and in particular the methanol/higher alcohol selectivity) during a long term test and to improve the understanding of deactivation features that affect the ternary catalyst at high temperature. In order to minimize the contribution of the formation of iron carbonyls upstream and deposition of iron onto the catalyst leading to the deactivation of the catalyst, special precautions were taken, and these included larger traps than the previous ones used, fresh activated charcoal and molecular sieve adsorbant materials was installed to purify the CO stream, and a water-cooling circuit was adopted to keep the reactant gas feed zone upstream from the copper-lined reactor in the temperature range of 40-70°C. In absence of a coolant, this zone (by conduction) reached 100-150°C when the reactor temperature was set to 340°C, thus favoring the formation of $Fe(CO)_5$. As usual, a copper-lined reactor was employed.

The catalyst stability experiment was carried out over a period of nearly 400 hr under the following higher alcohol synthesis conditions: GHSV = 5300 l/kg cat/hr, H_2/CO = 0.45, T = 340 °C, and P = 7.6 MPa. The trends of methanol and isobutanol productivity are plotted *vs* time of reaction in Figure 3.3.2.1. During the first 50 hr of reaction, a stable behavior of the catalyst was gradually reached. However, the overall activity of the catalyst was lower than expected on the basis of previous experiments. This was probably due to an incomplete degree of reduction of the catalyst. In fact, by gradually removing the CO reactant flow and maintaining the H_2 reactant flow for ≈10 hr (Event I in the figure), a full activity of the catalyst was subsequentely recovered with production of about 140 g/kg cat/hr of methanol and of 43.5 g/kg cat/hr of isobutanol (CO conversion was 14%).

During the following 300 hr of testing, a gradual loss of the catalyst activity toward higher alcohol synthesis, isobutanol as shown in Figure 3.3.2.1, was observed. As expected, the decreasing trend of CO conversion (equal to 8.5% at the end of the experiment) resulted in a gradually increasing formation rate of methanol, thermodynamically constrained to the gas phase composition. As shown in Figure 3.3.2.1, the catalyst activity trend was not drastically decreasing, but it was asymptotic with values of 170 g/kg cat/hr for the productivity of methanol and 22 g/kg cat/hr for the productivity of isobutanol, which was almost stable during the last 200 hr of reaction. Periodic increments of hydrogen partial pressure (in Figure 3.3.2.1, this is indicated as Events II, III, IV, and V where the CO flow was decreased for 3-8 hr to produce a H_2/CO ratio ≈ 5) yielded a temporary benefit to the catalytic activity, e.g. increments of 10-20% in isobutanol productivity accompanied by lowering of methanol productivity were observed after each treatment when testing was continued under the standard operating conditions.

Figure 3.3.2.1. Stability Data for the Cs/Cu/ZnO/Cr$_2$O$_3$ Catalyst at 340°C with H$_2$/CO = 0.45 Synthesis Gas at 7.6 MPa and GHSV = 5300 l/kg cat/hr
At events I-V, the synthesis gas mixture was changed to H$_2$/CO ≈ 5 for 3-8 hr by decreasing the CO flow rate (and thus the GHSV).

Productivity (g/kg cat/hr)

Hours on Stream

Productivity (g/kg cat/hr)

Hours on Stream
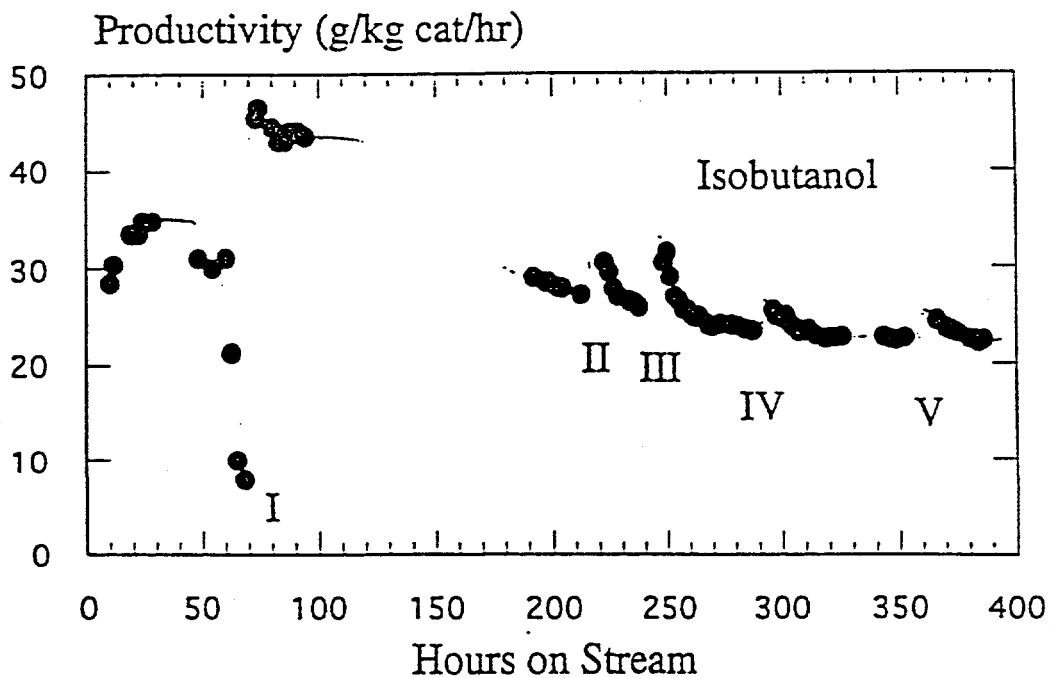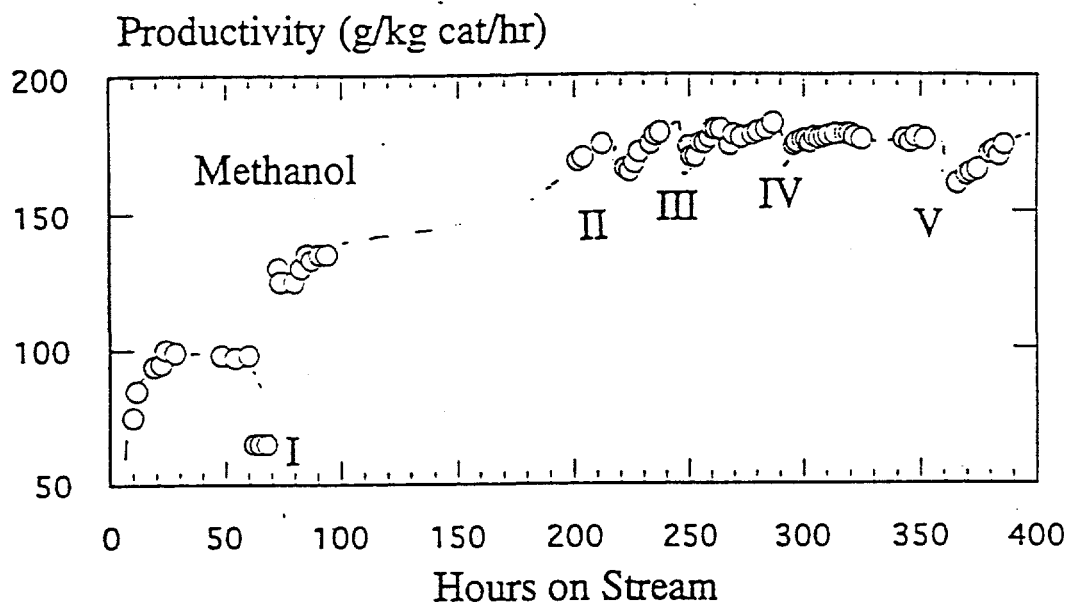
Characterization of this catalyst was carried out before and after testing, and some of the results are summarized here. The catalyst was prepared to give a nominal composition of Cu/Zn/Al = 30/45/25. Elemental analysis yielded the bulk metal ratio for the tested catalyst of 31.0/45.3/23.7. After Cs-doping and calcination at 350°C, the BET surface area was 86 m^2/g. The same surface area was obtained for the tested catalyst. The X-ray powder diffraction (XRD) pattern of the calcined sample showed that it was very poorly crystalline, as shown in Figure 3.3.2.2, where the broad peak at 2θ ≈42.5° corresponds to CuO. The XRD pattern for the tested catalyst showed the presence of more crystalline ZnO (but still small crystallite size) and metal Cu with a crystallite size ≤100 A, as indicated in Figure 3.3.2.2.

Even with the severe reaction temperature utilized in this experiment, the catalytic testing and characterization of this catalyst suggest that:

1) the state of reduction of the catalyst is critical for its activity and its stability,

2) the loss of activity observed at high temperature is in part reversible and recoverable by exposing the catalyst to an excess of hydrogen,

3) as a consequence of the H_2-rich treatments leading to higher activity, Cu° sintering, which is an irreversible process, cannot be the dominant or at least unique cause of the observed deactivation, and

4) the benefical effect of high H_2/CO feed ratios could be related to the catalyst state of reduction (perhaps not complete under the conditions employed nor stable for low values of hydrogen partial pressure) and/or to the presence of high molecular weight components (waxes) adsorbed on the catalyst surface and subsequent removed by H_2 (although the tested catalyst still exhibited a high surface area).

Figure 3.3.2.2. X-Ray Powder Diffraction Patterns of the Cs/Cu/ZnO/Cr$_2$O$_3$ Catalyst After Calcination and After Catalytic Testing

calcined — S.A.=86 m^2/g

tested — S.A.=86 m^2/g

crystal size ≤ 100 Å

2θ
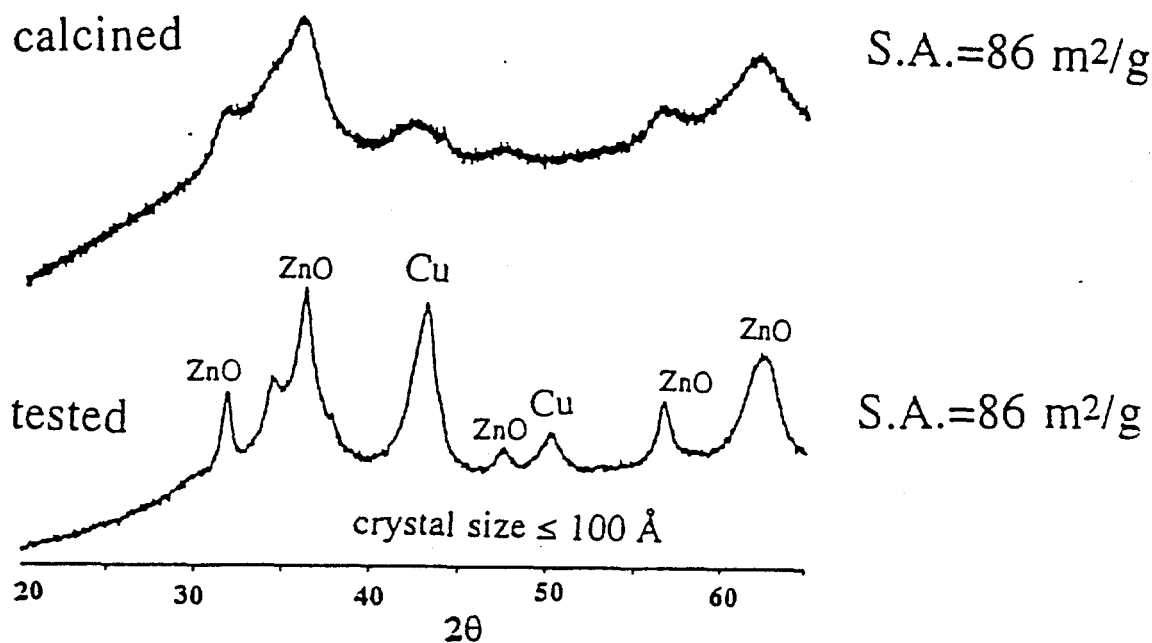
Further investigation of the performance of the Cs-promoted ternary Cu/ZnO/Cr$_2$O$_3$ catalyst was carried with respect to the effects that residence time and total pressure of the reactants exert on the production and distribution of methanol and higher alcohols. Kinetic runs have been performed at different values of gas hourly space velocity (GHSV) in the range of 3,300-18,300 l/kg cat/hr for two values of total pressure (7.6 and 6.5 MPa). The experiments were performed at the reaction temperature of 325°C and with a H$_2$/CO molar ratio equal to 0.75, which has already been reported to be optimal with respect to higher oxygenates.

It was observed that as the residence time increased, the productivity of methanol and linear alcohols decreased. However, as shown in Figure 3.3.2.3, this effect was less significant with the 2-methyl-1-propanol (isobutanol) product, especially at the lower pressure of 6.5 MPa. From Figure 3.3.2.3, it can be observed that:

- High space velocity values (short contact times) significantly favor the productivity of methanol, which reached over 1000 g/kg cat/hr.

- At the higher pressure, the productivity of all the higher oxygenates increases with increasing gas space velocity up to a maximum value beyond which further increments of space velocity make the residence time the limiting factor in the formation of higher alcohols (secondary products). An optimal production of oxygenates has been observed for GHSV = 12,000 l/kg

cat/hr, where the overall productivity of ethanol, propanol, and isobutanol approaches 250 g/kg cat/hr.

- At the lower pressure, the rate of formation of the linear and branched alcohols became slower at short contact times. On the contrary, at longer contact times (low space velocities), higher alcohol synthesis seems to be enhanced by lower reaction pressure. This comparison suggests that the formation of C_2+ oxygenates tends to slow down with increasing contact times at higher pressure, perhaps due to the inhibiting effect of adsorption phenomena that are expected to be more significant at high pressure. It is finally noted that at lower pressure, methanol formation is significantly reduced, and this provides high selectivities to higher oxygenates at longer residence times.

Figure 3.3.2.3. Effects of the Contact Time and the Total Pressure of the $H_2/CO = 0.75$ Synthesis Gas Reactant on the Productivities of the C_1-C_6 Alcohols at 325°C

Indicated are the linear and 2-methyl branched alcohols.

P=7.6 MPa   P=6.5 MPa

Productivity (g/kg cat/hr)

Contact Time (sec)
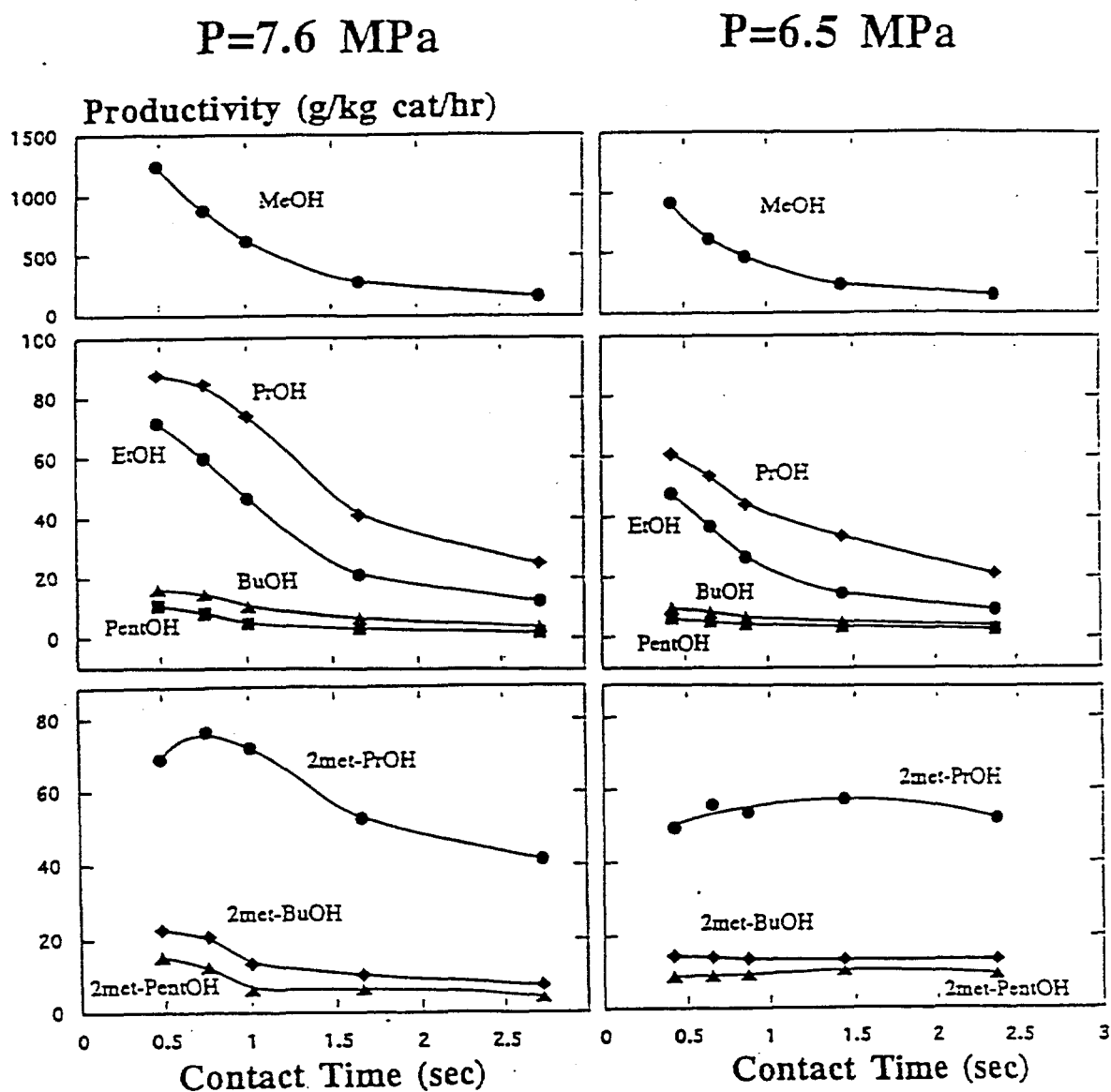
Cu/ZrO$_2$ Catalysts

Zirconia-based catalysts are being investigated for their potential as alcohol synthesis catalysts. In particular, a series of CuO/ZrO$_2$ catalysts having different Cu/Zr molar ratios have been prepared and initial characterization studies have been carried out with the precursors and the calcined oxides before catalytic testing is initiated.

The catalysts were prepared by aqueous coprecipatation at constant pH and temperature. A weighed quantity of Cu(NO$_3$)$_2$•2.5H$_2$O was dissolved in distilled water to make a 0.5 M solution. Similarly, a 0.5 M ZrO(NO$_3$)$_2$•6H$_2$O solution was prepared. These two solutions were mixed to give the desired Cu and Zr molar ratios of 10/90 and 30/70 in the final products. A basic buffer solution, used to control the pH, was prepared by mixing together 2 M sodium hydroxide and 2 M sodium acetate solutions.

Aqueous solutions of ZrO(NO$_3$)$_2$•6H$_2$O and Cu(NO$_3$)$_2$•2.5H$_2$O and of the buffer solution were poured into two separate dropping funnels. The reagents were added dropwise into a Pyrex flask containing 250 ml deionized water at 90°C that was vigorously stirred. The addition of these two solutions was adjusted to maintain the pH at about 7. Approximately 30 min was taken to complete the precipitation, and the resultant solid was allowed to digest for 45 min. The precipitate was then filtered and thoroughly washed with ≈4000 ml of warm deionized water. The color of the residue was deep blue. The dense mass was then dried in ambient atmosphere over a period of 48 hr. A significant amount of volume shrinkage occurred due to the loss of water and the color changed to dark blue. During filtration and washing, the wash water was not colored, indicating no loss of copper in this process. The precursors were crushed into pieces and kept at 110°C for another 24 hr to complete drying.

Separate samples of both of the precursors were calcined at 350°C, 400°C, and 500°C for 3 hr at each temperature. Surface area measurements (BET using N$_2$) were carried after calcination at the aforesaid temperatures. X-Ray powder diffraction patterns were obtained at each step to investigate the structural aspect of the material.

Significant surface areas were observed for the CuO/ZrO$_2$ = 10/90 mol% catalyst, as shown in Table 3.3.2.1. The surface areas for the 30/70 catalyst were lower but still appreciable. The dried precursors were X-ray amorphous, and the precursors calcined at 350°C and 400°C did not show the presence of crystalline components, as illustrated by Figure 3.3.2.4. However, precursors calcined at 500°C showed the presence of tetragonal ZrO$_2$, as indicated in Table 3.3.2.1 and in Figure 3.3.2.5. There was no evidence of crystalline CuO even after the precursors were calcined at 500°C. Dried precursors calcined at all these temperatures exhibited weight losses of about 16-18%.

Table 3.3.2.1. Surface Areas and X-ray Powder Diffraction Information for the CuO/ZrO_2 Materials After Calcination at 350, 400, and 500°C.

CuO/ZrO_2 Sample	Calcination Temperature	Surface area (m^2/g)	XRD Crystallinity
(10/90)	350°C	149	Amorphous
(10/90)	400°C	112	Amorphous
(10/90)	500°C	63	Tetragonal ZrO_2 CuO not detected
(30/70)	350°C	78	Amorphous
(30/70)	400°C	73	Amorphous
(30/70)	500°C	25	Tetragonal ZrO_2 CuO not detected

Overall 3QFY95 Objectives

Future plans for Task 3.3.2 will focus on the following areas:

(i)   To continue studies of increasing the conversion of H_2/CO to higher alcohols by promotion of the $C_1 \rightarrow C_2$ carbon chain growth step over Cs-promoted $Cu/ZnO/Cr_2O_3$ and MoS_2 catalysts,

(ii) To enhance the $C_2 \rightarrow C_3 \rightarrow C_4$ carbon chain growth steps over $Cs/Cu/ZnO/Cr_2O_3$ catalysts, and

iii) To prepare and test high surface area Cu/ZrO_2 catalysts, both Cs-doped and undoped, that are candidates for the synthesis of C_1-C_5 alcohols, in particular branched products such as isobutanol.

3.3.3   Study of Catalyst Preparation, Calcination, and Alkali Doping for Isobutanol Synthesis (University of Delaware)

Introduction

In this quarter, our study focused on the preparation, reaction testing, and characterization of the catalysts. By varying the factors, such as the basic precipitant (KOH instead of K_2CO_3), the calcination atmosphere (under nitrogen instead of air), and various dopant alkali metals, we were able to test for the sensitivity of isobutanol synthesis to these effects. The goal of these experiments is to improve isobutanol productivity from CO hydrogenation on our previously developed catalysts. From the following report, it is clearly seen that the KOH precipitation and nitrogen calcination significantly enhance the total alcohol productivity, and most importantly, the isobutanol selectivity. In addition, KOH precipitation leads to a suppression of n-propanol production, which is important since n-propanol is the major higher alcohol other than isobutanol produced on our catalysts. X-ray diffraction from the bulk structure of the new catalysts indicates no structurally significant feature that sets these materials apart from the previous